

Survey of experimental data

H. Oeschler

Institut für Kernphysik, Darmstadt University of Technology,
D-64289 Darmstadt, Germany

Abstract. A review of meson emission in heavy ion collisions at incident energies from SIS up to collider energies is presented. A statistical model assuming chemical equilibrium and local strangeness conservation (i.e. strangeness conservation per collision) explains most of the observed features.

Emphasis is put onto the study of K^+ and K^- emission at low incident energies. In the framework of this statistical model it is shown that the experimentally observed equality of K^+ and K^- rates at “threshold-corrected” energies $\sqrt{s} - \sqrt{s_{th}}$ is due to a crossing of two excitation functions. Furthermore, the independence of the K^+/K^- ratio on the number of participating nucleons observed between SIS and RHIC is consistent with this model.

It is demonstrated that the K^- production at SIS energies occurs predominantly via strangeness exchange and that this channel is approaching chemical equilibrium. The observed maximum in the K^+/π^+ excitation function is also seen in the ratio of strange to non-strange particle production. The appearance of this maximum around 30 $A \cdot \text{GeV}$ is due to the energy dependence of the chemical freeze-out parameters T and μ_B .

1. Introduction

Central heavy ion collisions at relativistic incident energies represent an ideal tool to study nuclear matter at high temperatures. Particle production is – at all incident energies – a key quantity to extract information on the properties of nuclear matter under these extreme conditions. Particles carrying strangeness have turned out to be very valuable messengers.

A specific purpose of this paper is the presentation of the evolution of strange particle production over a large range of incident energies. Many results are shown together with a theoretical interpretation. The attempts to describe particle production yields with statistical models [1-8] have turned out to be very successful over this large domain of incident energies.

2. General Trends

2.1. Production of pions and kaons from SIS to RHIC

At incident energies around 1 $A \cdot \text{GeV}$ pion and kaon production is very different: Pions can be produced by direct NN collisions in contrast to kaons. The threshold for K^+ production in NN collisions is 1.58 GeV and only collective effects can accumulate the energy needed to produce a K^+ together with a Λ due to strangeness conservation. The threshold for K^- production is even higher (2.5 GeV) as they are produced as $K^+ K^-$ pairs. These conditions lead to very different yields for the various mesons

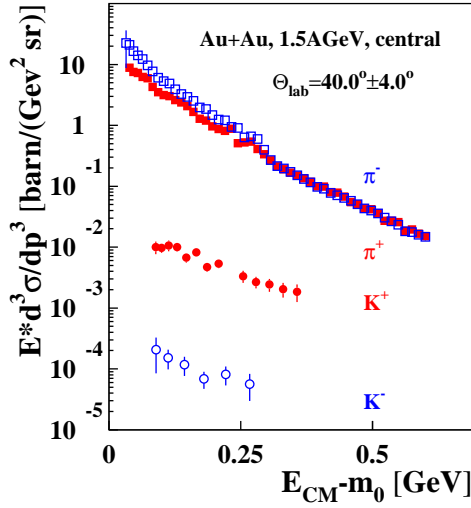


Figure 1. Spectra of positively and negatively charged pions and kaons measured in central collisions of Au+Au at 1.5 A-GeV. *Preliminary results.*

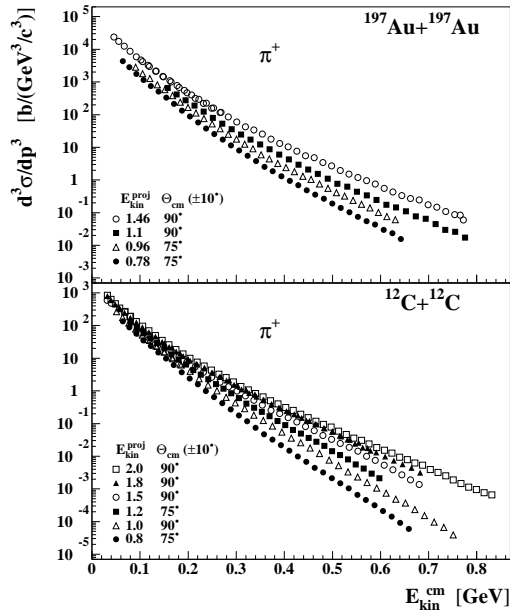


Figure 2. Spectra of positively charged pions in the center-of-mass frame close to midrapidity for Au+Au (upper part) and C+C (lower part). A deviation from a Boltzmann shape is seen at all incident energies and for both collision systems.

as demonstrated in Fig. 1 showing some spectra from central Au+Au collisions at 1.5 A-GeV. The yields of pions are much higher than for kaons; positively and negatively charged pions differ due to the N/Z ratio of Au. The yield of K^+ is by nearly two orders of magnitude higher than the one of K^- due to the different thresholds. At higher incident energies all these differences diminish as will be discussed.

Pion spectra of excellent quality are now available or will appear soon [9-10]. Figure 2 shows as an example spectra of positively charged pions as $d^3\sigma/dp^3$ (Boltzmann representation) for C+C and Au+Au collisions at different incident energies. The spectra are measured close to midrapidity.

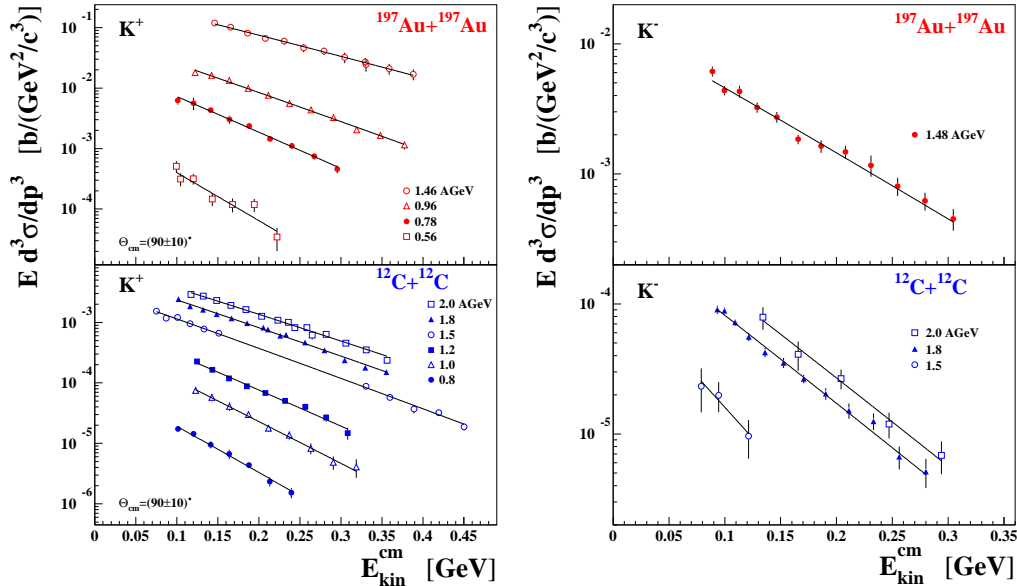


Figure 3. K^+ and K^- spectra measured at midrapidity for Au+Au (upper part) and C+C (lower part) at various incident energies [12, 13]. The spectra of K^- from Au+Au collisions are preliminary.

All spectra exhibit concave shapes in this representation deviating from a Boltzmann distribution which would be a straight line. Yet, even in a thermal condition one is not expecting a pure Boltzmann distribution as pions originate both from “free” pions and from resonance decay after freeze out. This type of shape is observed up to the highest incident energies and the above interpretation holds qualitatively. For a quantitative description with these two components still some work has to be done.

Spectra of K^+ and K^- from mass-symmetric systems C+C and Au+Au at incident energies from 0.6 to 2.0 A·GeV measured at midrapidity are shown in Fig. 3. They exhibit Boltzmann shapes in all cases [12, 13]. Their inverse slope parameters increase monotonously with incident energy and the heavier system exhibits harder spectra than the light system at the same incident energy.

The interaction of K^+ and K^- with nuclear matter is very different: Due to their \bar{s} content K^+ cannot be absorbed, while K^- can easily be absorbed on a nucleon converting it into a Λ . This difference makes the K^+ to be messengers of the early stage of the collision. Therefore K^+ are ideal probes for this dense stage and allow to extract the stiffness of the nuclear equation of state [13]. The basis of these studies is the ratio of K^+ measured in Au+Au and in C+C collisions as shown in Fig. 4. This subject is presented in detail in the talk by C. Sturm.

Figure 3 demonstrates that the yield of K^+ is much higher than the one of K^- as mentioned already. This is caused by the different production thresholds for K^+ and K^- . At AGS energies the ratio of K^+/K^- has decreased to about 5 [14] and is as low as 1.16 at RHIC [15]. This trend is summarized in Fig. 5. The dashed line represents the results of calculations using a statistical model [4, 5].

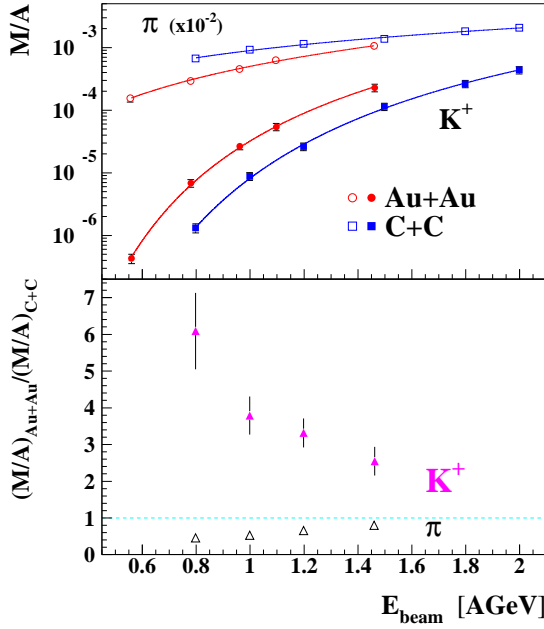


Figure 4. Upper part: Multiplicities of K^+ and pions per A as a function of incident energy. The pion data include charged and neutral pions. The lines represent fits to the data (see [13]). Lower part: Ratio of the multiplicities per A (Au+Au over C+C) as a function of incident energy.

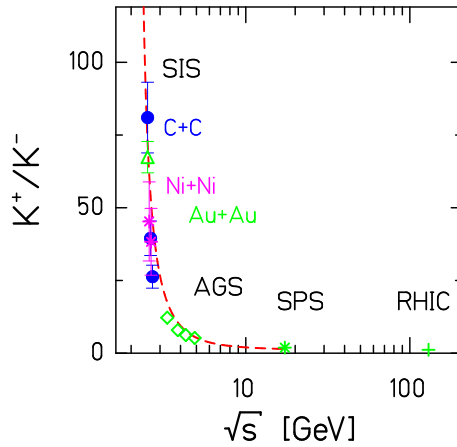


Figure 5. Ratio of positively and negatively charged kaons for various collisions systems from SIS up to RHIC. *Preliminary results.* The dashed line represents the results of calculations using the statistical model.

2.2. Interpretation within a statistical model

Pions and K^+ exhibit a further very pronounced contrast: While the pion multiplicity per number of participating nucleons A_{part} remains constant with A_{part} , the K^+ multiplicity per A_{part} rises strongly (Fig. 6). The latter observation seems to be in conflict with a thermal interpretation, which – in a naive view – should give multiplicities per mass number A being constant.

Usually, the particle number densities or the multiplicities per A_{part} , here for

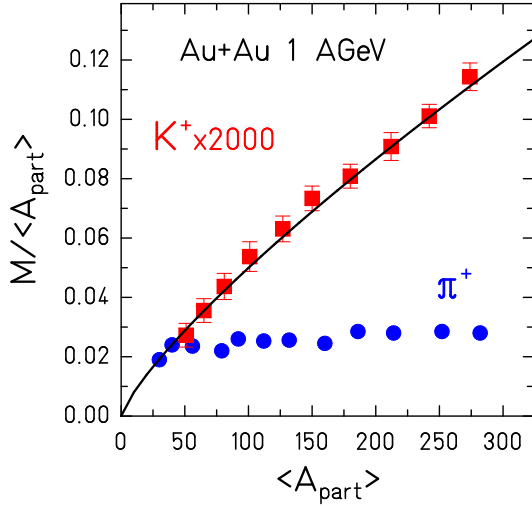


Figure 6. The multiplicity of K^+/A_{part} rises strongly with A_{part} in contrast to the pion multiplicity [17]. This rise can be described by the statistical model including local strangeness conservation (see text).

pions, are described in a simplified way by a Boltzmann factor

$$\frac{M_\pi}{A_{part}} \sim \exp\left(-\frac{\langle E_\pi \rangle}{T}\right),$$

with the temperature T and the total energy $\langle E_\pi \rangle$.

The production of strange particles has to fulfil strangeness conservation. The attempt to describe the measured particle ratios including strange hadrons at AGS and SPS using a strangeness chemical potential μ_S is quite successful [1, 2, 7, 8]. However, this grand-canonical treatment is not sufficient if the number of produced strange particles is small. Then a statistical model has to take care of *local strangeness conservation* in each reaction as introduced in [16]. This is done by taking into account that e.g. together with each K^+ a Λ or another strange particle is produced:

$$\frac{M_{K^+}}{A_{part}} \sim \exp\left(-\frac{\langle E_{K^+} \rangle}{T}\right) \left[g_\Lambda V \int \frac{d^3p}{(2\pi)^3} \exp\left(-\frac{(E_\Lambda - \mu_B)}{T}\right) \right],$$

where T is the temperature, μ_B the baryo-chemical potential, g_i the degeneracy factors, V the production volume for making the associate pair (see [4, 5]) and E_i the total energies. We note that this volume is not identical to the volume of the system at freeze out. The volume parameter V is taken as $r_V^3 A_{part}$ with a common $r_V = 1.07$ fm for all systems and all incident energies.

This formula, simplified for demonstration purposes, neglects other combinations leading to the production of K^+ as well as the use of Bose-Fermi distributions, which are all included in the computation. The corresponding formula for K^- production

$$\frac{M_{K^-}}{A_{part}} \sim \exp\left(-\frac{\langle E_{K^-} \rangle}{T}\right) \left[g_{K^+} V \int \frac{d^3p}{(2\pi)^3} \exp\left(-\frac{E_{K^+}}{T}\right) \right].$$

is similar, but does not depend on μ_B . This point will become important later on.

These formulae lead to a reduction of K^+ and K^- yields as compared to the numbers calculated without exact strangeness conservation [4, 5]. Two extreme conditions can be seen from these equations. In the limit of a small number of

strange particles the additional term (due to the parameter V) leads to a linear rise of M_{K^+}/A_{part} , while M_π/A_{part} remains constant. This is in very good agreement with the experimental observations shown in Fig. 6. For very high temperatures or very large volumina, the terms in brackets approach unity (see Ref. [4]) resulting in the grand-canonical formulation. This is much better seen in the exact formulae using modified Bessel functions [4, 5, 18].

At low incident energies, the particle ratios (except η/π_0) are well described using this canonical approach [4]. Surprisingly, even the measured K^+/K^- ratio is described and this ratio does not depend on the choice of the volume term V . It should be noted that the statistical model uses nominal masses of the particles while some transport calculations [19] have to reduce the K^- mass (as expected for kaon in the nuclear medium) in order to describe the measured yields.

Before comparing the data with the calculations in detail, a summary of the measurements by the KaoS Collaboration is given. These results have attracted considerable interest as in heavy ion collisions the K^- yield compared to the K^+ cross section is much higher than expected from NN collisions [12, 20]. This is especially evident if the kaon multiplicities are plotted as a function of $\sqrt{s} - \sqrt{s_{th}}$ where $\sqrt{s_{th}}$ is the energy needed to produce the respective particle in NN collisions taking into account the mass of the associate produced partner. To produce a K^+ in NN collisions $\sqrt{s_{th}} = 2.548$ GeV and a K^- $\sqrt{s_{th}} = 2.87$ GeV. The obvious contrast between NN and AA collisions, shown in Fig. 7, has led to the interpretation of the results by in-medium properties which cause e.g. a lower threshold for K^- production when produced in dense matter [19]. The observed difference between NN and AA collisions alone is not sufficient to conclude on properties of kaons in matter. In heavy ion collisions, kaons can be produced by other channels, e.g. $\pi\Lambda \rightarrow K^-N$ which are not available in NN collisions. Only by using detailed transport-model calculations one might conclude on new properties of kaons in matter [19].

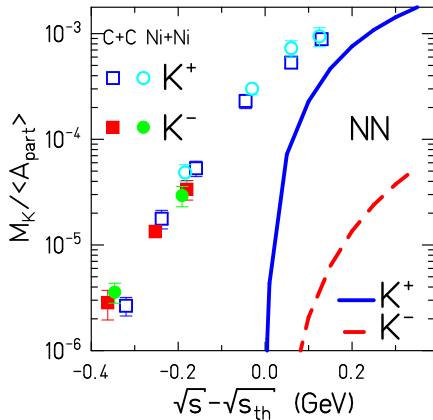


Figure 7. Measured K^+ and K^- yields in heavy ion and NN collisions as a function of $\sqrt{s} - \sqrt{s_{th}}$ [12, 20, 21]. $\langle A_{part} \rangle$ is $A/2$ for heavy ion data and 2 for NN collisions.

It is therefore of interest to see how the results of the statistical model appear in a representation where the K^+ and K^- multiplicities are given as a function of $\sqrt{s} - \sqrt{s_{th}}$. Figure 8 demonstrates that at values of $\sqrt{s} - \sqrt{s_{th}}$ less than zero the excitation functions for K^+ and K^- cross leading to the observed equality of K^+ and K^- at SIS energies. The yields differ at AGS energies by a factor of five. The difference in the rise of the two excitation functions can be understood by the formulae

given above. The one for K^+ production contains $(E_\Lambda - \mu_B)$ while the other has E_{K^+} in the exponent of the second term. As these two values are different, the excitation functions, i.e. the variation with T , exhibit a different rise.

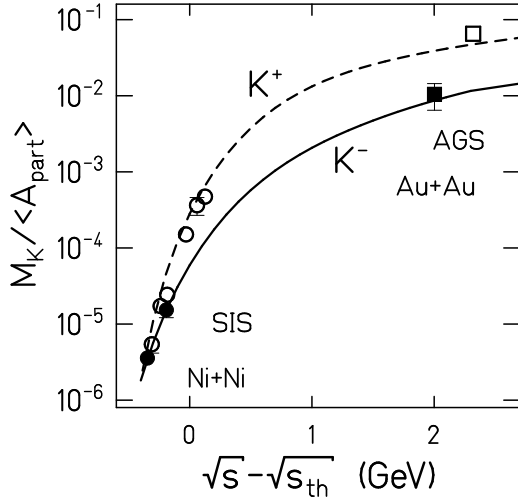


Figure 8. Calculated K^+/A_{part} and K^-/A_{part} ratios in the statistical model as a function of $\sqrt{s} - \sqrt{s_{th}}$ for Ni+Ni collisions. The points are results for Ni+Ni collisions at SIS energies [20, 21] and Au+Au at 10.2 A-GeV (AGS) [14]. At AGS energies the influence of the system mass is negligible.

Furthermore, the two formulae predict that the K^+/K^- ratio for a given collision should not vary with centrality as V cancels in the ratio. This has indeed been observed in Au+Au/Pb+Pb collisions between 1.5 A-GeV and RHIC energies [9, 15, 21, 14, 22] as shown in Fig. 9. This independence of centrality is most astonishing as one expects at low incident energies an influence of the different thresholds and the density variation with centrality. For instance at 1.93 A-GeV the K^+ production is above and the K^- production below their respective NN thresholds.

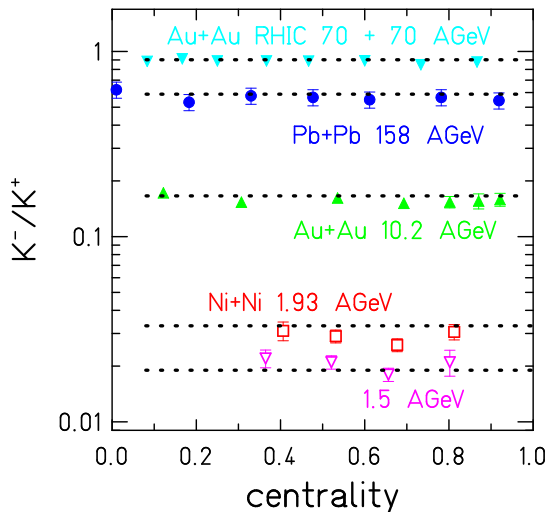
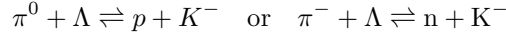


Figure 9. The K^+/K^- ratio appears to be constant as a function of centrality from SIS up to RHIC energies. The dotted lines represent the predictions of the statistical model. Data from [14, 15, 21].

Transport-model calculations show clearly that strangeness equilibration requires a time interval of 40 – 80 fm/c [23, 24]. On the other hand statistical models assuming chemical equilibration are quite successful in describing the particle yields including

strange particles.

In the case of K^+ production, no strong absorptive channel seems to be available which could lead to chemical equilibration. For K^- production the situation is quite different. At low incident energies strange quarks are found only in a few hadrons. The \bar{s} quark is essentially only in K^+ , while the s quark will be shared between K^- and Λ (or other hyperons). This sharing of the s quark might be in chemical equilibrium as the reactions



are strong and have only slightly negative Q-values of -176 MeV.

The idea that the K^- yield is dominated by strangeness exchange via the $\pi^- + \Lambda$ channel has been suggested by [25] and has been demonstrated quantitatively in a recent theoretical study [26]. The direct K^+K^- pair production via baryon-baryon collisions has negligible influence as these K^- are absorbed entirely. In these transport-model calculations the strangeness exchange is approaching equilibrium but does not fully reach it [26]. For details see the talk given by C. Hartnack.

If these reactions are the dominating channels, they might reach chemical equilibration, e.g. the rates for producing K^- and for absorbing K^- are equal. Then the law of mass action can be applied giving for the respective concentrations [27]

$$\frac{[\pi^{0,-}] \cdot [\Lambda]}{[K^-] \cdot N} = \kappa.$$

As the number of K^- relative to Λ is small, $[\Lambda]$ can be approximated by $[K^+]$ and rewriting gives

$$\frac{[K^-]}{[K^+]} \propto M(\pi^0 + \pi^-)/A_{part}.$$

This relation also explains that the measured ratio of K^-/K^+ is constant with centrality (Fig. 9) as the pion multiplicity does not vary with centrality. A detailed

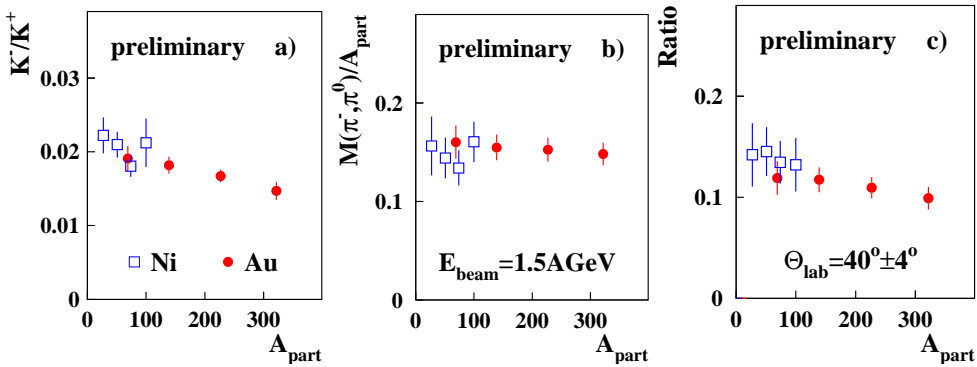


Figure 10. Measured K^-/K^+ ratio, $M(\pi^0 + \pi^-)/A_{part}$ and the double ratio $([K^-]/[K^+])/([M(\pi^0 + \pi^-)]/A_{part})$ as a function of A_{part} both for Ni+Ni and Au+Au collisions at 1.5 A·GeV. *Preliminary results.*

study for the low energies has been given in the talk by A. Förster. Figure 10 summarises by demonstrating the constancy of the K^-/K^+ ratio and of the pion multiplicity with A_{part} for Ni+Ni and Au+Au collisions at 1.5 A·GeV [9, 21, 28]. It turns out that these ratios do not even depend on the choice of the collision

system. The right part of this figure exhibits the double ratio $([K^-]/[K^+])/([M(\pi^0 + \pi^-)]/A_{part})$ which shows only a minor deviation from a horizontal line. This result can be taken as an argument that this specific channel is not far from chemical equilibrium.

Next we test in Fig. 11 the validity of the law of mass action by plotting the

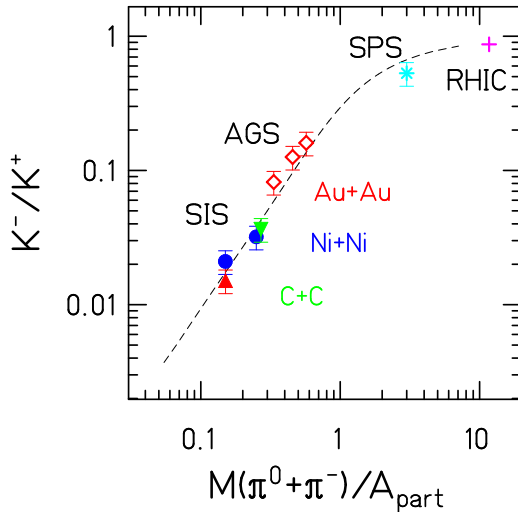


Figure 11. The K^-/K^+ ratio as a function of the pion multiplicity $M(\pi^0 + \pi^-)/A_{part}$ as a test of the law of mass action. *Preliminary data.* The dashed line shows the prediction of the statistical model.

K^-/K^+ ratio as a function of the pion multiplicity $M(\pi^0 + \pi^-)/A_{part}$ at incident energies from SIS up to RHIC. At SIS and AGS energies the direct relation holds, i.e. the K^-/K^+ ratio rises with $M(\pi^0 + \pi^-)/A_{part}$. At SPS and RHIC energies the linear relation is no longer valid; K^- are obviously produced by other channels, i.e. K^+K^- pair production. This change of the dominating channel is well reproduced by the statistical model (dashed line in Fig. 11).

2.3. Maximum relative strangeness content in heavy ion collisions around 30 A·GeV

The experimental data from heavy ion collisions show that the K^+/π^+ ratio rises from SIS up to AGS but it is larger for AGS than at the highest CERN-SPS energies [3, 14, 22, 29, 30] and decreases even further at RHIC [15] as shown in Fig. 12.

This behavior is of particular interest as it could signal the appearance of new dynamics for strangeness production in high energy collisions. It was even conjectured [31] that this property could indicate an energy threshold for quark-gluon plasma formation in relativistic heavy ion collisions. Some transport models are able to describe the occurrence of this maximum within a continuous evolution of hadron rescattering and string degrees of freedom [32].

In the following we analyze the energy dependence of strange to non-strange particle ratios in the framework of a hadronic statistical model. In the whole energy range, the hadronic yields observed in heavy ion collisions resemble those of a population in chemical equilibrium along a unified freeze-out curve determined by the condition of fixed energy/particle $\simeq 1$ GeV [3] providing a relation between the temperature T and the baryon chemical potential μ_B . As the beam energy increases T rises and μ_B is slightly reduced. Above AGS energies T exhibits only a moderate change and converges to its maximal value in the range of 160 to 180 MeV, while μ_B is strongly decreasing.

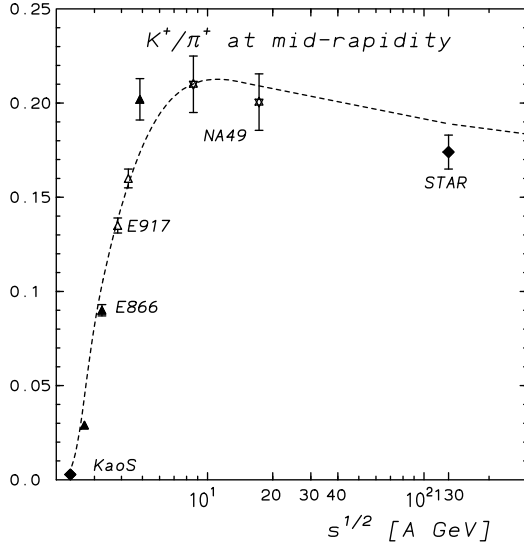


Figure 12. K^+/π^+ ratio obtained around midrapidity as a function of \sqrt{s} from the various experiments. The dashed line shows the results of the statistical model in complete equilibrium.

Instead of studying the K^+/π^+ ratio we use the ratios of strange to non-strange particle multiplicities (Wroblewski factor) [33] defined as

$$\lambda_s \equiv \frac{2\langle s\bar{s} \rangle}{\langle u\bar{u} \rangle + \langle d\bar{d} \rangle}$$

where the quantities in angular brackets refer to the number of newly formed quark-antiquark pairs, i.e. it excludes all quarks that were present in the target and the projectile.

Applying the statistical model to particle production in heavy ion collisions calls for the use of the canonical ensemble to treat the number of strange particles particularly for data in the energy range from SIS up to AGS [4, 34] as mentioned before. The calculations for Au-Au and Pb-Pb collisions are performed using a canonical correlation volume defined above. The quark content used in the Wroblewski factor is determined at the moment of *chemical freeze-out*, i.e. from the hadrons and especially, hadronic resonances, before they decay. This ratio is thus not an easily measurable observable unless one can reconstruct all resonances from the final-state particles. The results are shown in Fig. 13 as a function of \sqrt{s} .

The solid line (marked “sum”) in Fig. 13 describes the statistical-model calculations in complete equilibrium along the unified freeze-out curve [3] and with the energy-dependent parameters T and μ_B . From Fig. 13 we conclude that around 30 A-GeV laboratory energy the relative strangeness content in heavy ion collisions reaches a clear and well pronounced maximum. The Wroblewski factor decreases towards higher incident energies and reaches a limiting value of about 0.43. For details see Ref. [35].

The appearance of the maximum can be traced to the specific dependence of μ_B and T on the beam energy. Figure 14 shows lines of constant λ_s in the $T - \mu_B$ plane. As expected λ_s rises with increasing T for fixed μ_B . Following the chemical freeze-out curve, shown as a dashed line in Fig. 14, one can see that λ_s rises quickly from SIS to AGS energies, then reaches a maximum at $\mu_B \approx 500$ MeV and $T \approx 130$ MeV. These freeze-out parameters correspond to 30 A-GeV laboratory energy. At higher incident

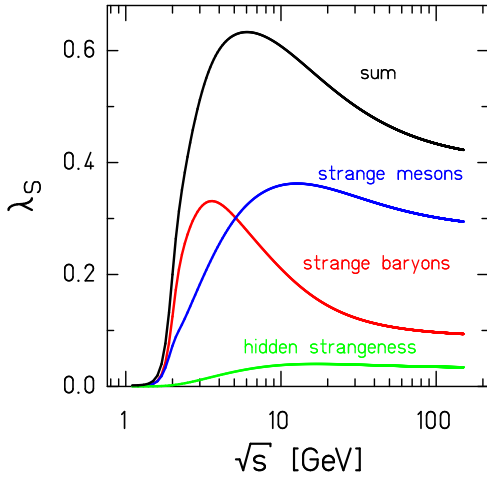


Figure 13. Contributions to the Wroblewski factor λ_s (for definition see text) from strange baryons, strange mesons, and mesons with hidden strangeness. The sum of all contributions is given by the full line.

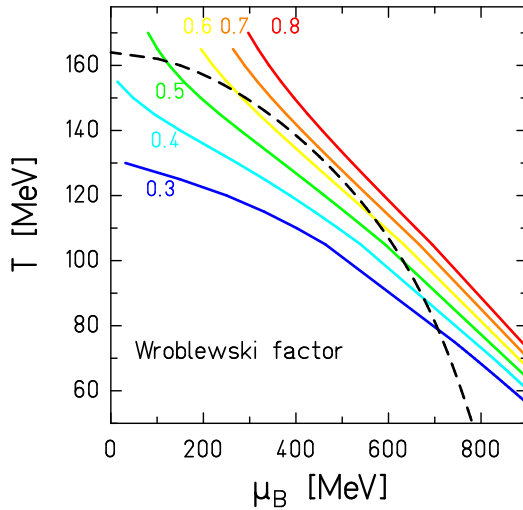


Figure 14. Lines of constant Wroblewski factor λ_s (for definition see text) in the $T - \mu_B$ plane (solid lines) together with the freeze-out curve (dashed line) [3].

energies the increase in T becomes negligible but μ_B keeps on decreasing and as a consequence λ_s also decreases.

The importance of finite baryon density on the behavior of λ_s is demonstrated in Fig. 13 showing separately the contributions to $\langle s\bar{s} \rangle$ coming from strange baryons, from strange mesons and from hidden strangeness, i.e. from hadrons like ϕ and η . As can be seen in Fig. 13, the origin of the maximum in the Wroblewski ratio can be traced to the contribution of strange baryons. This channel dominates at low \sqrt{s} and loses importance at high incident energies. Even strange mesons exhibit a broad maximum. This is due to the presence of associated production of e.g. kaons together with hyperons.

The energy dependence of the K^+/π^+ ratio measured at midrapidity is shown in Fig. 12. The model gives an excellent description of the data, showing a broad maximum at the same energy as the one seen in the Wroblewski factor. In general, statistical-model calculations should be compared with 4π -integrated results since

strangeness does not have to be conserved in a limited portion of phase space. A drop in this ratio for 4π yields has been reported from preliminary results of the NA49 collaboration at 158 A-GeV [29]. This decrease is, however, not reproduced by the statistical model without further modifications, e.g. by introducing an additional parameter $\gamma_s \sim 0.7$ [6]. This point might be clearer when data at other beam energies will become available.

3. Summary

Strange particle production in heavy ion collisions over a rather broad range of incident energies can be described by a statistical model. The production of strange particles close to threshold requires a canonical formulation, i.e. local strangeness conservation. This approach is able to explain many features of K^+ and K^- production at SIS energies.

While for K^+ production it remains open whether and how chemical equilibrium can be reached, the situation is quite different for K^- . It is shown that the strangeness exchange process $\pi\Lambda \rightleftharpoons N + K^-$ is the dominant channel for K^- production at SIS and likely also at AGS energies. This is demonstrated by applying the corresponding law of mass action. Theoretical studies confirm this interpretation.

Using the energy dependence of the parameters T and μ_B we have shown that the statistical-model description of relativistic heavy ion collisions predicts that the yields of strange to non-strange particles reaches a well defined maximum near 30 GeV lab energy. It is demonstrated that this maximum is due to the specific shape of the freeze-out curve in the $T - \mu_B$ plane. In particular a very steep decrease of the baryon chemical potential with increasing energy causes a corresponding decline of relative strangeness content in systems created in heavy ion collisions above lab energies of 30 GeV. The saturation in T , necessary for this result, might be connected to the fact that hadronic temperatures cannot exceed the critical temperature $T_c \simeq 170$ MeV for the phase transition to the QGP as found in solutions of QCD on the lattice.

In spite of the apparent success of the statistical models it should not appear the impression that these models describe everything. They describe yields, particle ratios. Looking at spectral shapes already the expansion dynamics shows up. The distribution of the particles in space is a very informative quantity as e.g. [36]. The description of this quantity is beyond statistical models.

It is a pleasure for me to thank for the stimulating collaboration with P. Braun-Munzinger, J. Cleymans, K. Redlich, and the whole KaoS Crew (I. Böttcher, A. Förster, E. Grosse, P. Koczoń, B. Kohlmeyer, F. Laue, M. Menzel, L. Naumann, F. Pühlhofer, E. Schwab, P. Senger, Y. Shin, H. Ströbele, F. Uhlig, A. Wagner, W. Waluś).

- [1] J. Cleymans and H. Satz, Z. Phys. **C57** (1993) 135.
- [2] P. Braun-Munzinger, J. Stachel, J.P. Wessels and N. Xu, Phys. Lett. B **344** (1995) 43; Phys. Lett. B **365** (1996) 1.
- [3] J. Cleymans and K. Redlich, Phys. Rev. Lett. **81** (1998) 5284; Phys. Rev. **C60** (1999) 054908.
- [4] J. Cleymans, H. Oeschler, K. Redlich, Phys. Rev. **C59** (1999) 1663.
- [5] J. Cleymans, H. Oeschler, K. Redlich, Phys. Lett. **485** (2000) 27.
- [6] F. Becattini, J. Cleymans, A. Keränen, E. Suhonen and K. Redlich, Phys. Rev. **C64** (2001) 024901.
- [7] P. Braun-Munzinger, I. Heppe, J. Stachel, Phys. Lett. B **465** (1999) 15.
- [8] P. Braun-Munzinger, D. Magestro, K. Redlich, J. Stachel, Phys. Lett. B **518** (2001) 41.
- [9] A. Förster, Ph.D.Thesis, Darmstadt University of Technology, in preparation.

- [10] J. Klay, Ph.D.Thesis, University of California, Davis, 2001.
- [11] A. Mischke, this conference.
- [12] F. Laue, C. Sturm et al., Phys. Rev. Lett. 82 (1999) 1640.
- [13] C. Sturm et al., Phys. Rev. Lett. 86 (2001) 39; C. Sturm, Ph.D.Thesis, Darmstadt University of Technology, 2001.
- [14] L. Ahle et al., (E-802 Collaboration), Phys. Rev. **C58** (1998) 3523; Phys. Rev. C60 (1999) 044904; L. Ahle et al., E866/E917 Collaboration, Phys. Lett. B476 (2000) 1; Phys.Lett. B490 (2000) 53.
- [15] J. Harris, (STAR Collaboration), Talk presented at QM2001, Stony Brook, January 2001, Nucl. Phys. A (2001) (in print).
- [16] R. Hagedorn, CERN Yellow Report 71-12 (1971); E. Shuryak. Phys. Lett. **B42** (1972) 357; J. Rafelski, Phys. Lett. **B97** (1980) 297; K. Redlich and L. Turko, *Z. Phys. C* **5**, 1980 (201); R. Hagedorn et al., *Z. Phys.* **C27** (1985) 541.
- [17] M. Mang, Ph.D.Thesis, University of Frankfurt, 1997.
- [18] J. S. Hamieh, K. Redlich and A. Tounsi, Phys. Lett. **B486** (2000) 61.
- [19] W. Cassing et al., Nucl. Phys. **A614** (1997) 415.
- [20] R. Barth et al., Phys. Rev. Lett. 78 (1997) 4007.
- [21] M. Menzel, Ph.D.Thesis, Universität Marburg, 2000.
- [22] J.C. Dunlop and C.A. Ogilvie, Phys. Rev. C61 (2000) 031901 and references therein; C. A. Ogilvie. Talk presented at QM2001, Stony Brook, January 2001, Nucl. Phys. A (2001) (in print). nucl-th/9911015; J.C. Dunlop, Ph.D.Thesis, MIT, 1999.
- [23] P. Koch, B. Müller and J. Rafelski, Phys. Rep. **142** (1986) 167.
- [24] E.L. Bratkovskaya et al., Nucl. Phys. **A675** (2000) 661.
- [25] C. M. Ko, Phys. Lett. B138 (1984) 361.
- [26] C. Hartnack, H. Oeschler, J. Aichelin, nucl-th/0109016.
- [27] H. Oeschler, J. Phys. G: Nucl. Part. Phys. 27 (2001) 1.
- [28] F. Uhlig, Ph.D.Thesis, Darmstadt University of Technology, in preparation.
- [29] Ch. Blume, NA49 Collaboration. Talk presented at QM2001, Stony Brook, January 2001, Nucl. Phys. A (2001) (in print).
- [30] I. Bearden, NA44 Collaboration, Phys. Lett. B471 (1999) 6.
- [31] M. Gaździcki and M. Gorenstein, Acta Phys. Pol. B30 (1999) 2705; M. Gaździcki and D. Röhrich, *Z. Phys.* **C71** (1996) 55.
- [32] F. Wang et al., Phys. Rev. C61 (2000) 064904; and contribution to this volume.
- [33] A. Wroblewski, Acta Physica Polonica B16 (1985) 379.
- [34] C.M. Ko, V. Koch, Z. Lin, K. Redlich, M. Stephanov and X.N. Wang, Phys. Rev. Lett. 86 (2001) 5438.
- [35] P. Braun-Munzinger, J. Cleymans, H. Oeschler, K. Redlich, Nucl. Phys. A 697 (2002) 902.
- [36] Y. Shin et al., Phys. Rev. Lett. 81 (1998) 1576.